Pharm Res (2010) 27:2715–2724
DOI 10.1007/s11095-010-0272-x

RESEARCH PAPER

Lipophilicity and Transporter Influence on Blood-Retinal Barrier Permeability: A Comparison with Blood-Brain Barrier Permeability

Ken-ichi Hosoya • Atsushi Yamamoto • Shin-ichi Akanuma • Masanori Tachikawa

Received: 17 July 2010 / Accepted: 2 September 2010 / Published online: 22 September 2010

ABSTRACT

Purpose To determine the lipophilicity trend line from the relationship between the blood-retinal barrier (BRB) permeability and the lipophilicity of permeants and compare it with that of the blood-brain barrier (BBB).

Methods The retinal (RUI) and brain uptake index (BUI) of 26 radiolabeled compounds across the rat BRB and BBB, respectively, were measured using the carotid artery injection method.

Results RUI was determined using 13 compounds expected to be transported from blood to the retina by passive diffusion and with a log *n*-octanol/Ringer distribution coefficient (DC) ranging from −2.56 to 2.48. The RUI values were correlated with the log of the DC [RUI = 46.2 × exp (0.515 × log DC), $r^2 = 0.807$]. A similar trend was obtained between BUI and lipophilicity. The RUI value for substrates of the influx transporters and P-glycoprotein (P-gp) was greater and smaller than the lipophilicity trend line, respectively. In contrast, [^{3}H]verapamil, which is a substrate of P-gp, has a greater RUI value than the lipophilicity trend line, but not for BUI, suggesting that the BRB has an influx transport system for verapamil.

Conclusions The lipophilicity trend line constructed from the RUI and DC values is considered to reflect the transport properties of drugs undergoing passive diffusion across the BRB.

KEY WORDS blood-brain barrier · blood-retinal barrier · lipophilicity · P-glycoprotein · transporter

K.-i. Hosoya (✉) · A. Yamamoto · S.-i. Akanuma · M. Tachikawa
Department of Pharmaceutics
Graduate School of Medicine and Pharmaceutical Sciences
University of Toyama
Toyama, Japan
e-mail: hosoyak@pha.u-toyama.ac.jp

INTRODUCTION

Drug delivery to the retina from the circulating blood is limited by the membrane permeability of the blood-retinal barrier (BRB), which forms complex tight junctions of retinal capillary endothelial cells (inner BRB) and retinal pigment epithelial cells (outer BRB) (1,2). Understanding the barrier and transport functions at the BRB, as well as the physicochemical and biological factors that control solute transfer, is important for the design of drug delivery systems to the retina and for preventing entry into the neural retina to avoid unexpected side effects. Although the paracellular transport of drugs across both the endothelium and epithelium is prevented by these tight junctions, the permeability of the BRB varies considerably depending on the properties of drugs and the conditions of the BRB (1,3).

The BRB efficiently supplies nutrients to the retina and removes endobiotics and xenobiotics from the retina to maintain a constant milieu in the neural retina (4). Recent progress in BRB research has revealed that retinal capillary endothelial and retinal pigment epithelial cells express several influx and efflux transporters, such as facilitative glucose transporter 1 (GLUT1/Slc2a1), Na^+-dependent multivitamin transporter (SMVT/Slc5a6), L (leucine-referring) amino acid transporter 1 (LAT1/Slc7a5), cationic amino acid transporter 1 (CAT1/Slc7a1), organic anion transporter 3 (OAT3/Slc22a8), P-glycoprotein (P-gp/mdr1/ABCB1), multidrug resistance protein 4 (MRP4/ABCC4), and breast cancer resistance protein (BCRP/ABCG2) (2,5–11). Thus, it is known that nutrients, such as D-glucose, vitamins, and amino acids, cross the BRB (5–8). It is also believed that lipophilic compounds cross the BRB. Although Kadam and Kompella reported that *in vitro n*-octanol/Ringer distribution coefficients (DC) of drugs can be predicted to *in vivo* retinal distribution of drugs after *trans*-scleral delivery (12), there are no reports on

systematic BRB permeability estimates from lipophilicity. The lipophilicity trend line produced as an indication of the relationship between transport from the blood to the retina and the lipophilicity of permeants is important to predict BRB permeability form *in vitro* DC of drugs and to compare the transporter-mediated transport.

In the brain, the blood-brain barrier (BBB) is structurally similar to the inner BRB and limits drug transport from the circulating blood to the brain (13). Several research groups have demonstrated that the BBB permeability of permeants is proportional to their lipophilicity (13–15). Lipophilicity trend lines are available, and it is possible to predict the BBB permeability of certain drugs from their lipophilicity.

The purpose of this study was to determine the lipophilicity trend line estimated from the relationship between the BRB permeability and lipophilicity of permeants. The BRB permeability was measured for 26 radiolabeled compounds using the carotid artery injection method and compared with their BBB permeability.

MATERIALS AND METHODS

Animals

Male Wistar rats, weighing 250–300 g, were purchased from Japan SLC (Hamamatsu, Japan). The investigations using rats described in this report conformed to the provisions of the Animal Care Committee, University of Toyama, and the ARVO Statement on the Use of Animals in Ophthalmic and Vision Research.

Reagents

p-[glycyl-2-^{3}H]-Aminohippuric acid ([^{3}H]PAH, 4.04 Ci/mmol), d-[8,9-^{3}H(N)]biotin ([^{3}H]biotin, 60 Ci/mmol), [1,2,6,7-^{3}H(N)]-corticosterone ([^{3}H]corticosterone, 78.5 Ci/mmol), [^{3}H(G)]-digoxin ([^{3}H]digoxin, 35.4 Ci/mmol), 3,4-[ring-2,5,6-^{3}H]-dihydroxyphenylethylamine ([^{3}H]dopamine, 54.2 Ci/mmol), [^{3}H]H_2O (1.0 mCi/g), L-[4,5-^{3}H(N)]-leucine ([^{3}H]L-leucine, 59.2 Ci/mmol), D-[1-^{3}H(N)]mannitol ([^{3}H]D-mannitol, 14.2 Ci/mmol), α-[1-^{14}C]methylaminoisobutyric acid ([^{14}C]MeAIB, 50.5 mCi/mmol), [1,2,6,7-^{3}H(N)]-testosterone ([^{3}H]testosterone, 70.0 Ci/mmol), L-[3′,5′-^{125}I]-thyroxine, ([^{125}I]T_4, 4400 Ci/mmol), and [5,6-^{3}H]-uracil ([^{3}H]uracil, 31.9 Ci/mmol) were purchased from Perkin-Elmer Life and Analytical Sciences (Boston, MA). [N-methyl-^{3}H] Acetyl-L-carnitine hydrochloride ([^{3}H]acetyl-L-carnitine, 85 Ci/mmol), [N-methyl-^{14}C]antipyrine ([^{14}C]antipyrine, 55 mCi/mmol), L-[2,3-^{3}H]arginine ([^{3}H]L-arginine, 50.6 Ci/mmol), n-[1-^{14}C]butanol ([^{14}C]butanol, 5 mCi/mmol), [4-^{14}C]creatinine ([^{14}C]creatinine, 55 mCi/mmol), [N-methyl-^{14}C]diazepam ([^{14}C] diazepam, 55 Ci/mmol), L-3,4-[ring2,5,6-^{3}H]dihydroxyphenylalanine, ([^{3}H]L-Dopa, 60 Ci/mmol), [1,2,6,7-^{3}H]progesterone ([^{3}H]progesterone, 101.3 Ci/mmol), [N-methyl ^{3}H]verapamil hydrochloride ([^{3}H]verapamil, 80 Ci/mmol), and [^{3}H(G)]vincristine sulfate ([^{3}H]vincristine, 10 Ci/mmol) were purchased from American Radiolabeled Chemicals (St. Louis, MO). D-[2-^{3}H(N)] Glucose ([^{3}H]D-glucose, 8.4 Ci/mmol), [4,5-^{3}H]valproic acid ([^{3}H]valproic acid, 51.0 Ci/mmol), and (RS)-[phenyl-4-^{3}H]warfarin ([^{3}H]warfarin, 17.4 Ci/mmol) were obtained from Moravek Biochemicals (Brea, CA) and [2,8-^{3}H] adenosine ([^{3}H]adenosine, 35.9 Ci/mmol), [U-^{14}C]glycine ([^{14}C]glycine, 101 mCi/mmol), and L-[2,6-^{3}H]phenylalanine ([^{3}H]L-phenylalanine, 54.0 Ci/mmol) were obtained from GE Healthcare (Piscataway, NJ). All other chemicals were of reagent grade and available commercially.

Carotid Artery Injection Method

Carotid artery injections were performed in rats to measure the retinal (RUI) and brain uptake index (BUI) of radiolabeled compounds (16–18). Briefly, rats were anesthetized with an intraperitoneal injection of sodium pentobarbital (60 mg/kg), and then a 200 μL injection solution was injected into the common carotid artery. The injection solution consisted of Ringer-Hepes buffer (141 mM NaCl, 4 mM KCl, 2.8 mM $CaCl_2$, 10 mM Hepes, pH 7.4) which contained both 5 μCi [^{3}H]test compound, and 1 μCi [^{14}C]butanol as a highly diffusible reference in the presence or absence of inhibitors. When the test compound is in the [^{14}C] or [^{125}I] form (1 μCi), [^{3}H]H_2O (5 μCi) is used as a highly diffusible reference. Rats were decapitated 0.25 min after injection, and the retina and cerebrum were removed. The retina and cerebrum were dissolved in 2 N NaOH and subsequently neutralized. After double-isotope liquid-scintillation counting with quench correction (LSC-5000, Aloka, Tokyo, Japan), the RUI and BUI values for the [^{3}H], [^{14}C], and [^{125}I] form of the test compound was calculated (16–18). For RUI and BUI for the [^{3}H] form of the test compound,

$$\mathrm{RUI} = ([^{3}\mathrm{H}]/[^{14}\mathrm{C}](\mathrm{dpm\ in\ the\ retina}))/([^{3}\mathrm{H}]/[^{14}\mathrm{C}](\mathrm{dpm\ in\ the\ injectate})) \times 100 \quad (1)$$

$$\mathrm{BUI} = ([^{3}\mathrm{H}]/[^{14}\mathrm{C}](\mathrm{dpm\ in\ the\ cerebrum}))/([^{3}\mathrm{H}]/[^{14}\mathrm{C}](\mathrm{dpm\ in\ the\ injectate})) \times 100 \quad (2)$$

RUI and BUI express the fractional uptake of the [^{3}H] form of the test compound as a percentage of the fractional uptake of the reference compound [^{14}C]butanol in the retina and brain, respectively.

For RUI and BUI for the [^{14}C] or [^{125}I] form of the test compound,

$$\text{RUI} = ([^{14}\text{C}] \text{ or } [^{125}\text{I}]/[^{3}\text{H}](\text{dpm in the retina}))/ ([^{14}\text{C}]\text{or}[^{125}\text{I}]/[^{3}\text{H}] \text{ (dpm in the injectate)}) \times 100 \quad (3)$$

$$\text{BUI} = ([^{14}\text{C}]\text{or}[^{125}\text{I}]/[^{3}\text{H}](\text{dpm in the cerebrum}))/ ([^{14}\text{C}]\text{or}[^{125}\text{I}]/[^{3}\text{H}](\text{dpm in the injectate})) \times 100 \quad (4)$$

RUI and BUI express the fractional uptake of the [^{14}C] or [^{125}I] form of the test compound as a percentage of the fractional uptake of the reference compound [^{3}H]H_2O in the retina and brain, respectively.

In order to estimate extraction of reference compounds by the retina and brain at 0.25 min after injection, the elimination rate constant (k) of reference compounds was measured. At 0.25, 0.5, 1.0, 3.0 min after injection of 1 μCi [^{14}C]butanol or 5 μCi [^{3}H]H_2O, rats were decapitated, the retina and cerebrum were removed, and radioactivity was measured as described above. The change in retina and brain content of the reference compounds with time is described (19):

$$E(t) = [E(0)]e^{-kt} \quad (5)$$

where E(t) is the extraction by the retina or brain at 0.25 min after injection, E(0) is the initial or maximal extraction [E(0) = 1], and t is the time after carotid injection. Extraction (E_d) by the retina ($E_{d,\ retina}$) and brain ($E_{d,\ brain}$) of the test compound by the retina or brain was calculated as follows:

$$E_{d,\ retina} = \text{RUI}/100 \times E_{but(0.25)} \text{ or } E_{H_2O(0.25)} \quad (6)$$

$$E_{d,\ brain} = \text{BUI}/100 \times E_{but(0.25)} \text{ or } E_{H_2O(0.25)} \quad (7)$$

where $E_{but(0.25)}$ or $E_{H_2O(0.25)}$ is the extraction of the reference compound, [^{14}C]butanol or [^{3}H]H_2O at 0.25 min after injection, respectively. The permeability-surface-area product (PS) of the retina (PS_{BRB}) or brain (PS_{BBB}) for the test compound is determined from the following relationship (18,20):

$$PS_{BRB} = -F \times \ln (1 - E_{d,\ retina}/100) \quad (8)$$

$$PS_{BBB} = -F \times \ln (1 - E_{d,\ brain}/100) \quad (9)$$

where F is the retinal blood flow, which is 0.70 mL/(min·g retina) for the rat retina (21) or the cerebral blood flow, which is 0.81 mL/(min·g brain) for the rat brain (18).

Determination of Distribution Coefficients

The DC of radiolabeled compounds between *n*-octanol/Ringer-Hepes buffer (pH 7.4) was determined as described previously (12,22). Briefly, the buffer and *n*-octanol were mutually saturated by shaking at 37°C for 16 h. The DC at 37°C was determined by incubating 1 mL the equilibrated buffer containing radiolabeled test compound with 1 mL of *n*-octanol for 24 h to reach distribution equilibrium. At the end of 24 h, the *n*-octanol and buffer phase were separated by centrifugation, and the radioactivity of test compound in both phases was measured in a liquid scintillation counter (LSC-5000, Aloka).

$$\text{DC} = \text{dpm per g } n\text{-octanol/dpm per g buffer} \quad (10)$$

Data Analysis

Unless otherwise indicated, all data represent means ± SEM. An unpaired, two-tailed Student's *t*-test was used to determine the significance of differences between two groups.

RESULTS

Relationship Between Retinal Uptake Index and Lipophilicity

To determine the effects of lipophilicity on drug transport across the BRB and BBB, we measured the RUI and BUI for 13 radiolabeled compounds which are expected to be transported from the blood to the retina by passive diffusion and with a log DC ranging from −2.56 to 2.48 (Table I) and results are shown in Fig. 1. The RUI values of [^{3}H]D-mannitol and [^{3}H]MeAIB were used from our previous reports (23,24). The RUI values increased with increasing log DC and ranged from 11.6% to 235%. The estimated regression line is RUI = 46.2 × exp (0.515 × log DC) as a lipophilicity trend line for BRB permeability. This correlation between RUI and log DC was significant ($r^2 = 0.807$, $p < 0.01$) (Fig. 1a). A similar relationship was obtained between the BUI and log DC. The BUI values ranged from 2.99% to 166%. The estimated regression line is BUI = 24.2 × exp (0.816 × log DC) as a lipophilicity trend line for BBB permeability. This correlation between BUI and log DC was significant ($r^2 = 0.885$, $p < 0.01$) (Fig. 1b). In a comparison between RUI and BUI values, hydrophilic compounds (log DC < −1), such as [^{14}C]MeAIB, [^{3}H]PAH, [^{3}H]D-mannitol, [^{14}C]creatinine, and [^{3}H]dopamine, have 3- to 5-fold greater RUI values than BUI values, whereas for lipophilic compounds (log DC > 0), such as [^{3}H]valproic acid, [^{14}C]

Table I The BRB and BBB Permeability of Compounds with Different Lipophilicities and Transport Properties

Compounds	Characteristics	DC	Log DC	RUI (%)	$E_{d,\ retina}$ (%)	Log (PS_{BRB}) (mL/(min·g retina))	BUI (%)	$E_{d,\ brain}$ (%)	Log (PS_{BBB})(mL/(min·g brain))
[^{14}C]Diazepam	Passive	303	2.48	136 ± 8	124 ± 8	-	166 ± 2	147 ± 1	-
[^{3}H]Progesterone	Passive	99.0	2.00	235 ± 28	222 ± 27	-	119 ± 3	107 ± 2	-
[^{3}H]Testosterone	Passive	84.2	1.93	142 ± 2	135 ± 2	-	138 ± 9	124 ± 8	-
[^{3}H]Corticosterone	Passive	31.8	1.50	96.5 ± 3.0	91.4 ± 2.9	0.253 ± 0.071	82.0 ± 4.0	74.0 ± 3.6	0.0390 ± 0.0443
[^{3}H]Warfarin	Passive	5.87	0.769	34.0 ± 6.0	32.2 ± 5.7	-0.579 ± 0.096	33.0 ± 3.8	29.8 ± 3.4	-0.548 ± 0.058
[^{14}C]Antipyrine	Passive	2.12	0.326	136 ± 2	125 ± 1	-	138 ± 5	123 ± 5	-
[^{3}H]Valproic acid	Passive	1.91	0.280	50.4 ± 5.8	47.7 ± 5.5	-0.348 ± 0.068	80.5 ± 3.5	72.6 ± 3.1	0.0226 ± 0.0390
[^{3}H]Dopamine	Passive	0.0955	-1.02	21.8 ± 0.9	20.6 ± 0.9	-0.793 ± 0.021	4.98 ± 0.18	3.22 ± 0.12	-1.43 ± 0.02
[^{3}H]Uracil	Passive	0.0790	-1.10	65.6 ± 5.1	62.2 ± 4.9	-0.168 ± 0.058	5.93 ± 0.76	5.34 ± 0.69	-1.36 ± 0.05
[^{14}C]Creatinine	Passive	0.00861	-2.06	16.0 ± 2.0	14.7 ± 1.8	-0.964 ± 0.057	4.01 ± 0.50	3.57 ± 0.44	-1.54 ± 0.06
[^{3}H]D-Mannitol	Passive	0.00609	-2.22	11.6 ± 1.4[a]	11.0 ± 1.3	-1.09 ± 0.06	3.11 ± 0.28	2.80 ± 0.25	-1.64 ± 0.04
[^{3}H]PAH	Passive	0.00455	-2.34	15.7 ± 0.2	14.8 ± 1.5	-0.957 ± 0.051	2.99 ± 0.21	2.70 ± 0.19	-1.66 ± 0.03
[^{14}C]MeAIB	Passive	0.00278	-2.56	12.6 ± 2.7[b]	11.6 ± 2.5	-1.09 ± 0.11	3.69 ± 0.32	3.28 ± 0.28	-1.57 ± 0.04
[^{125}I]T_4	Oatp1c1	91.2	1.96	61.3 ± 6.8	56.2 ± 6.2	-0.242 ± 0.083	31.1 ± 3.2	27.7 ± 2.8	-0.598 ± 0.053
[^{3}H]Adenosine	ENT2	0.0924	-1.03	32.3 ± 2.8[a]	30.6 ± 2.6	-0.605 ± 0.044	9.51 ± 1.34	8.58 ± 1.21	-1.17 ± 0.06
[^{3}H]Acethyl-L-carnitine	OCTN2	0.0632	-1.20	18.0 ± 1.3[c]	17.1 ± 1.2	-0.900 ± 0.035	4.99 ± 0.47[c]	4.50 ± 0.42	-1.46 ± 0.05
[^{3}H]L-Dopa	LAT1	0.0600	-1.22	95.7 ± 7.0	90.6 ± 6.6	0.219 ± 0.108	58.0 ± 3.9	52.3 ± 3.5	-0.223 ± 0.043
[^{3}H]L-Phenylalanine	LAT1	0.0550	-1.26	117 ± 4	111 ± 4	-	76.2 ± 5.9	68.8 ± 5.3	-0.0238 ± 0.0646
[^{3}H]L-Leucine	LAT1	0.0375	-1.43	95.3 ± 1.1	90.2 ± 1.0	0.213 ± 0.021	39.4 ± 6.8	35.5 ± 6.1	-0.464 ± 0.090
[^{3}H]Biotin	SMVT	0.00628	-2.20	31.7 ± 3.9[d]	30.0 ± 3.7	-0.620 ± 0.069	11.4 ± 1.3	10.3 ± 1.2	-1.07 ± 0.05
[^{3}H]L-Arginine	CAT1	0.00511	-2.29	204 ± 18	193 ± 17	-	33.8 ± 6.4	30.5 ± 5.8	-0.551 ± 0.096
[^{3}H]D-Glucose	GLUT1	0.00152	-2.82	75.7 ± 2.2	71.7 ± 2.1	-0.0527 ± 0.0255	38.7 ± 4.2	34.9 ± 3.8	-0.465 ± 0.056
[^{14}C]Glycine	GlyT1	0.00106	-2.98	21.6 ± 1.8[b]	19.7 ± 1.7	-0.817 ± 0.042	3.04 ± 0.22	2.71 ± 0.19	-1.66 ± 0.03
[^{3}H]Vincristine	P-gp	138	2.14	50.0 ± 1.8	47.4 ± 1.7	-0.348 ± 0.022	43.2 ± 0.7	38.9 ± 0.7	-0.399 ± 0.010
[^{3}H]Digoxin	P-gp	26.1	1.42	60.9 ± 3.1	57.7 ± 2.9	-0.221 ± 0.035	2.86 ± 0.22	2.58 ± 0.20	-1.68 ± 0.03
[^{3}H]Verapamil	P-gp	8.18	0.913	391 ± 34	370 ± 32	-	32.5 ± 5.7	29.4 ± 5.1	-0.570 ± 0.092

Each value represents the mean ± S.E.M. (n = 3-9). The distribution coefficient (DC) of each compound between n-octanol and Ringer-Hepes buffer (pH 7.4) was determined in this study. [a] Nagase *et al.* (23); [b] Okamoto *et al.* (24);[c] Tachikawa *et al.* (25); [d] Ohkura *et al.* (6); PAH, *p*-aminohippuric acid; MeAIB, α-methylaminoisobutyric acid; T_4, thyroxine.

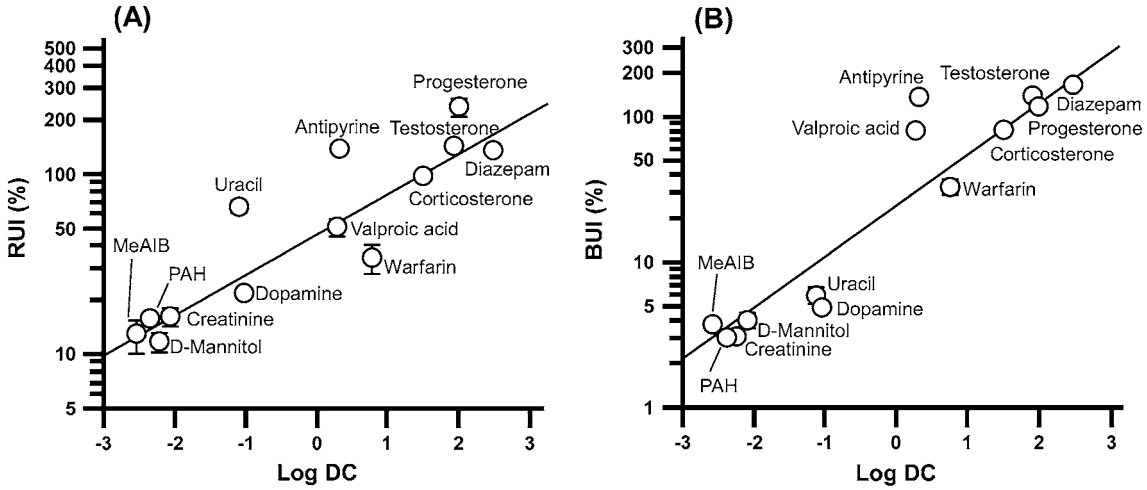

Fig. 1 Correlation of the retinal (RUI) (**A**) and brain uptake index (BUI) (**B**) and the *n*-octanol/Ringer distribution coefficient (DC) in rats. For these thirteen compounds, an exponential relationship is described by the equation RUI = 46.2 × exp(0.515 × log DC) ($r^2 = 0.807$, $p < 0.01$) (**A**) and BUI = 24.2 × exp(0.816 × log DC) ($r^2 = 0.885$, $p < 0.01$) (**B**). Each point represents the mean ± SEM ($n = 3$–9). PAH, *p*-aminohippuric acid; MeAIB, α-methylaminoisobutyric acid.

antipyrine, [^{3}H]warfarin, [^{3}H]corticosterone, [^{3}H]testosterone, and [^{14}C]diazepam, the values are almost the same (Table I).

Relationship Between Permeability-Surface Product of BRB and Lipophilicity

After carotid artery injection of [^{14}C]butanol or [^{3}H]H_2O, the elimination constant, k, was calculated from the % remaining in the retina or brain *vs* time profile. [^{14}C]Butanol was exponentially eliminated from the retina and brain, and k was 0.218±0.083 min^{-1} for the retina and 0.413± 0.019 min^{-1} for the brain (data not shown). The $E_{but(0.25)}$ in the retina and brain was found to be 0.947 and 0.902, respectively, using Eq 5. In the exponential elimination of [^{3}H]H_2O in the retina and brain, k was 0.350±0.051 min^{-1} for the retina and 0.469±0.060 min^{-1} for the brain (data not shown). The $E_{H_2O(0.25)}$ in the retina and brain was found to be 0.916 and 0.889, respectively, using Eq. 5.

The direct relationship between the BUI and permeability of the BBB can be obtained by application of the Crone equation (Eq. 9, (20)). We hypothesized that the permeability of the BRB can be obtained from the RUI value by this equation (Eq. 8). Confirmation of this hypothesis was sought by obtaining estimates of the PS_{BRB} and attempting to correlate the PS_{BRB} with distribution coefficients and comparing this with a correlation of the PS_{BBB} with distribution coefficients (Table I). Of the 13 radiolabeled compounds undergoing passive diffusion, [^{3}H]progesterone, [^{14}C]diazepam, [^{3}H]testosterone, and [^{14}C]antipyrine were omitted when plotting the PS_{BRB} or PS_{BBB} *vs* distribution coefficients because the $E_{d,\ retina}$ and $E_{d,\ brain}$ were more than 100%. As demonstrated in Fig. 2a, log PS_{BRB} exhibits a linear relationship with the log DC. In this instance, log $PS_{BRB} = -0.382 + 0.263 \times \log DC$ describes the statistically significant ($r^2 = 0.706$, $p < 0.01$) correlation between these parameters. A similar result was obtained between log PS_{BBB} and log DC: log $PS_{BBB} = -0.647 + 0.442 \times \log DC$ ($r^2 = 0.861$, $p < 0.01$) (Fig. 2b).

Comparison of Retinal Uptake Index Relationships in Transporters and the Lipophilicity Trend Line

In order to determine the effect of influx and efflux transporters on BRB and BBB permeability, the RUI and BUI of substrates of solute carrier (SLC) transporters and P-gp were examined (Fig. 3 and Table I). The RUI values of [^{3}H]biotin, [^{3}H]adenosine, [^{3}H]acetyl-L-carnitine, and [^{14}C]glycine and the BUI value of [^{3}H]acetyl-L-carnitine were taken from our previous reports (6,23–25). For the compounds expected to undergo influx transport by SLC transporters, the RUI and BUI values of [^{3}H]L-arginine, [^{3}H]D-glucose, [^{3}H]L-Dopa, [^{3}H]biotin, [^{3}H]L-leucine, and [^{3}H]L-phenylalanine were more than 2.84-fold greater than the lipophilicity trend line which was estimated from Fig. 1. The RUI and BUI values of [^{14}C]glycine were 2.17- and 1.41-fold greater than the lipophilicity trend line, respectively. The RUI and BUI values of [^{3}H]adenosine were placed on the lipophilicity trend line, whereas the RUI and BUI values of [^{3}H]acetyl-L-carnitine and [^{125}I]T_4 were lower than the lipophilicity trend line. To confirm the involvement of a transporter for [^{3}H]L-Dopa and [^{3}H]L-arginine, an inhibition study was carried out (Table II). In the presence of 10 mM L-Dopa and L-arginine, the RUI values of [^{3}H]L-Dopa and [^{3}H]L-arginine were reduced by 30.1% and 70.3%, and the BUI values were reduced by

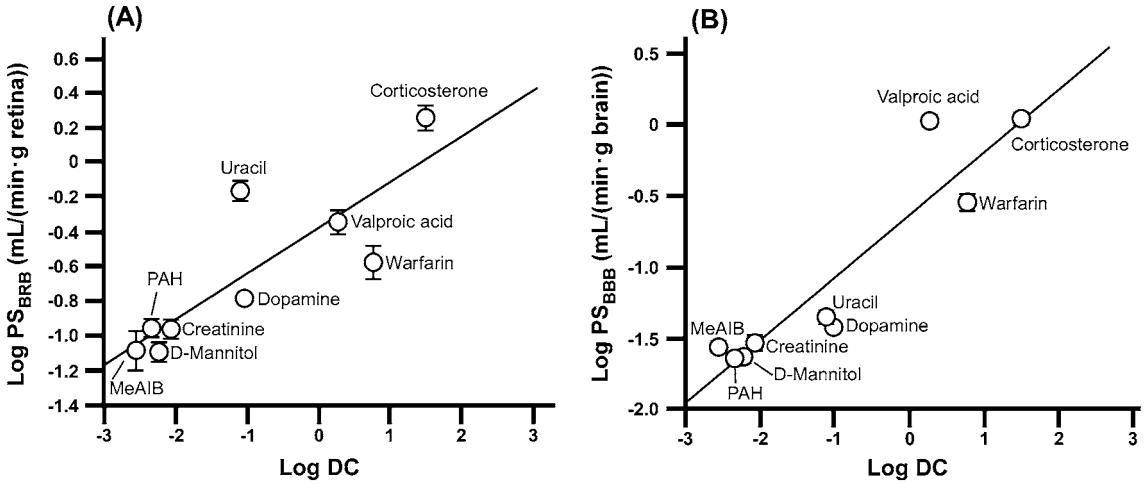

Fig. 2 Correlation of the permeability-surface area product of the retina (PS_{BRB}) (**A**) and brain (PS_{BBB}) (**B**) and the *n*-octanol/Ringer distribution coefficient (DC) in rats. For these nine compounds, a linear relationship is described by the equation $\log PS_{BRB} = -0.382 + 0.263 \times \log DC$ ($r^2 = 0.706$, $p < 0.01$) (**A**) and $\log PS_{BBB} = -0.647 + 0.442 \times \log DC$ ($r^2 = 0.861$, $p < 0.01$) (**B**). Each point represents the mean ± SEM ($n = 3$–9). PAH, *p*-aminohippuric acid; MeAIB, α-methylaminoisobutyric acid.

69.6% and 83.9%, respectively. These results support the hypothesis that L-Dopa and L-arginine undergo influx transport by LAT1 and CAT1, respectively, at the BRB and BBB (7,8,26,27). In the case of [^{125}I]T_4, the BUI value was reduced by 47.7% in the presence of 50 μM T4, whereas the RUI value was not changed. The BUI value of [^{14}C] glycine was unchanged in the presence of 10 mM glycine.

For the compounds expected to undergo efflux transport by P-gp, the RUI and BUI values of [^{3}H]digoxin and [^{3}H] vincristine were lower than the lipophilicity trend line. To confirm the involvement of a transporter for [^{3}H]digoxin, an inhibition study using a P-gp inhibitor was carried out (Table II). Although the RUI and BUI values of [^{3}H] digoxin exhibited little change in the presence of 10 μM digoxin, these values were increased to 142% and 197%, respectively, in the presence of 5 mM verapamil, supporting the hypothesis that digoxin undergoes efflux transport by P-gp at the BRB and BBB. Interestingly, although the BUI

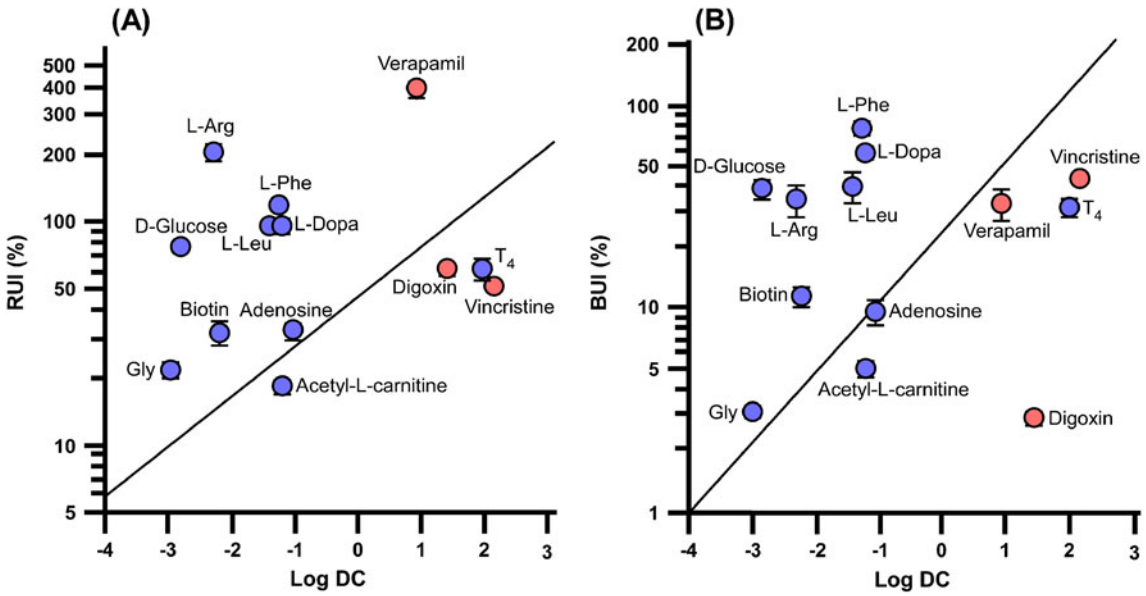

Fig. 3 Comparison of the retinal (RUI) (**A**) and brain uptake index (BUI) (**B**) relationship in transporters and the lipophilicity trend line. The lipophilicity trend line indicates the correlation between the RUI (**A**) and BUI (**B**) and the log DC of the thirteen compounds in Fig. 1. Blue and red circles are substrates for SLC transporters and P-gp, respectively. Each point represents the mean ± SEM ($n = 3$–6). L-Arg, L-arginine; L-Phe, L-phenylalanine; L-Leu, L-leucine; Gly, Glycine; T_4, thyroxine.

Table II The Effect of Inhibitors on the Retinal and Brain Uptake Index for Substrates of Transporters in Rats

Compounds	Inhibitors	RUI (%)	% of control	BUI (%)	% of control
[^{3}H]L-Dopa		95.7 ± 7.0	100 ± 7	58.0 ± 3.9	100 ± 7
	10 mM L-Dopa	66.8 ± 3.0*	69.9 ± 3.1*	17.7 ± 1.3*	30.4 ± 2.3*
[^{3}H]L-Arginine		204 ± 18	100 ± 9	33.8 ± 6.4	100 ± 19
	10 mM L-Arginine	60.5 ± 3.0*	29.7 ± 1.5*	5.43 ± 0.61*	16.1 ± 1.8*
[^{14}C]Glycine		-	-	3.04 ± 0.22	100 ± 7
	10 mM Glycine	-	-	3.08 ± 0.21	101 ± 7
[^{125}I]T_4		61.3 ± 6.8	100 ± 5	31.1 ± 3.2	100 ± 10
	50 μM T_4	72.5 ± 8.3	118 ± 14	16.3 ± 1.3*	52.3 ± 4.2*
[^{3}H]Digoxin		60.9 ± 3.1	100 ± 5	2.86 ± 0.22	100 ± 8
	5 mM Verapamil	86.7 ± 2.8*	142 ± 5*	5.62 ± 0.87**	197 ± 30**
[^{3}H]Digoxin†		56.2 ± 10.8	100 ± 19	2.00 ± 0.07	100 ± 4
	10 μM Digoxin†	54.7 ± 2.0	97.3 ± 3.6	1.65 ± 0.08*	82.5 ± 3.8*

Each value represents the mean ± S.E.M. (n = 3-9). † Ringer-Hepes buffer containing 0.1% dimethyl sulfoxide was used in this study.

*$p < 0.01$; **$p < 0.05$, significantly different from control. T_4, thyroxine

value of [^{3}H]verapamil was lower than the lipophilicity trend line, the RUI value of [^{3}H]verapamil was 5.29-fold greater than the lipophilicity trend line.

DISCUSSION

The present study clearly shows that the lipophilicity trend line estimated from the RUI and DC values can be considered as an indication of the transport properties of drugs across the BRB. Moreover, the demonstration that the lipophilic properties of compounds undergoing passive diffusion could be correlated with equal facility to the RUI or the PS_{BRB} suggests that estimations of BRB permeability can be derived from RUI measurements as is the case for BBB permeability (13–15). This contrasts with studies involving relatively larger RUI values compared with BUI values showing that the BRB is more permeable than the BBB. In addition, the uptake index of glycine, T_4, and verapamil, which are expected to exhibit transporter-mediated transport, is different in the BRB and BBB, suggesting that the BRB has different *in vivo* transport functions involving transporter-mediated transport compared with the BBB.

Alm *et al.* first demonstrated that the BRB permeation of nutrients could be evaluated by an RUI study as is the case for BBB permeation by a BUI study (16,17). The present study extends this observation to include a wide variety of compounds. [^{3}H]PAH and [^{14}C]MeAIB are substrates of OAT3 and system A (ATA2/Slc38a2), respectively, which are expressed at the inner BRB and exhibit an uptake function at the abluminal (retinal) side (9,28). Thus, both compounds are most likely transported via passive diffusion in the blood-to-retina/vitreous humor direction (24,29). We found using several compounds undergoing passive diffusion that the RUI values correlated with the lipophilicity (log DC), and the same was true for the observed BUI *vs* log DC (Fig. 1). These results support the hypothesis that the lipophilicity of compounds is correlated with the BRB permeability as is the case for the BBB permeability. Indeed, the PS_{BRB} of several compounds has a less than 100% $E_{d,\,retina}$ correlation with log DC, and the same was true for the observed PS_{BBB} *vs* log DC (Fig. 2). The lipophilicity trend line is able to predict the BRB permeability of permeants from their DC if permeants cross the BRB via passive diffusion.

Although the RUI values for hydrophilic compounds (log DC < −1), such as [^{14}C]MeAIB, [^{3}H]PAH, [^{3}H]D-mannitol, [^{14}C]creatinine, and [^{3}H]dopamine, are mostly 3- to 5-fold greater than the corresponding BUI values, the RUI values for lipophilic compounds (log DC > 0), such as [^{3}H]valproic acid, [^{14}C]antipyrine, [^{3}H]warfarin, [^{3}H]corticosterone, [^{3}H]testosterone, and [^{14}C]diazepam, are almost the same as the BUI values (Table I). These results suggest that paracellular transport by the BRB for hydrophilic compounds is greater than that of the BBB, and the transcellular transport of lipophilic compounds by the BRB is the same as that by the BBB. This is in agreement with the results of Ennis and Betz (30) and Stewart and Tuor (3). They reported using intravenous and carotid artery injection techniques in the rat that the BRB permeability of [^{14}C]sucrose and [^{14}C]α-amino-isobutyric acid is about 4-fold greater than that of the BBB (3,30). Although the contribution of the outer BRB to the retinal transfer of compounds at the BRB is unclear, Stewart and Tuor used electron micrographs of the rat inner BRB and BBB to show that retinal vessels have a higher number of interendothelial junctions than those of the brain, suggesting that the inner BRB exhibits a higher paracellular transport than the BBB (3). Thus, permeability for paracellular transport between the endothelial cells of the inner BRB is several times greater than that of the BBB, although the inner BRB has a similar structure to the BBB. Further studies are needed to investigate the contribution of the outer BRB to total BRB transport.

The RUI and BUI values of [^{3}H]progesterone, [^{3}H]diazepam, [^{3}H]testosterone, and [^{14}C]antipyrine were more than 100%, suggesting that efflux from the retina and brain of these compounds is slower than that of reference compounds. It appears that these lipophilic compounds bind to some protein in the retina and/or brain after transport from the blood and, thus, apparently exhibit an extraction greater than 100%.

Although [^{3}H]L-arginine, [^{14}C]glycine, [^{3}H]D-glucose, [^{3}H]L-Dopa, [^{3}H]L-leucine, [^{3}H]L-phenylalanine, [^{3}H]biotin, [^{3}H]acetyl-L-carnitine, and [^{3}H]adenosine are hydrophilic compounds (log DC<-1.0), their RUI values, except for [^{3}H]acetyl-L-carnitine, are greater than the lipophilicity trend line (Fig. 3a). CAT1, glycine transporter 1 (GlyT1/Slc6a9), GLUT1, LAT1, SMVT, and equilibrative nucleoside transporter 2 (ENT2/Slc29a2) are expressed at the inner BRB and contribute blood-to-retina transport of their substrates (5–8,23–25). The BUI values of [^{3}H]L-arginine, [^{3}H]D-glucose, [^{3}H]L-Dopa, [^{3}H]biotin, [^{3}H]L-leucine, and [^{3}H]L-phenylalanine are also greater than the lipophilicity trend line (Fig. 3b). CAT1, GLUT1, LAT1, and SMVT are expressed at the BBB and contribute the blood-to-brain transport of their substrates (26,27,31,32), although the glycine transporter does not function at the BBB due to a failure of self-inhibition in the BUI study of [^{14}C]glycine (Table II). These findings support the idea that the uptake of [^{3}H]L-arginine and [^{3}H]L-Dopa by the retina and brain is inhibited in the presence of 10 mM L-arginine and L-Dopa (Table II). In addition to [^{3}H]L-arginine and [^{3}H]L-Dopa, we have reported that the uptake of [^{14}C]glycine, [^{3}H]biotin, and [^{3}H]adenosine by the retina is inhibited in the presence of an excess of each compound (6,23,24). This evidence supports the demonstration that the RUI value of substrates of SLC transporters is greater than the lipophilicity trend line. Many patients with Parkinson's disease have blurred vision or other visual disturbances, which are reflected in the reduced retinal dopamine concentration and delayed visual evoked potentials (33). L-Dopa corrects these deficiencies (34). LAT1 at the BRB is important for drug delivery to the retina as well as LAT1 at the BBB (35). However, the RUI and BUI values of [^{3}H]acetyl-L-carnitine are lower than the lipophilicity trend line (Fig. 3a and b), although the retinal uptake of [^{3}H]acetyl-L-carnitine, but not the brain uptake, was inhibited in the presence of 2 mM acetyl-L-carnitine and L-carnitine (25). The lack of agreement between the lower RUI value of [^{3}H]acetyl-L-carnitine and self-inhibition need to be explained. It appears that Na^+-dependent organic cation/carnitine transporter 2 (OCTN2/Slc22a5) and some efflux transport process acts on the influx and efflux transport of acetyl-L-carnitine at the BRB at the same time. The RUI and BUI values of [^{3}H]adenosine were almost on the lipophilicity trend line, although the retinal uptake of [^{3}H]adenosine was inhibited in the presence of 2 mM adenosine (23). ENT2 most likely mediates adenosine at the inner BRB (23). The adenosine concentration in the rat retina/choroid (36) (approximately 0.9 nmol/g≈0.9 μM) is about 10-fold greater than that in the blood (90 nM) (37). Therefore, the net efflux of adenosine transport at the inner BRB may occur as at the BBB (37), since ENT2 is a bi-directional equilibrative transporter.

T_4 is expected to be transported by a transporter from the blood to the retina or brain because T_4 is an essential constituent in the retina and brain as a thyroid hormone (38). The BUI value of [^{125}I]T_4 was reduced in the presence of 50 μM T_4, but the RUI value was not (Table II). Although this is in agreement with T_4 transport by organic anion transporting polypeptide 1c1 (oatp1c1/oatp14/Slco1c1) at the BBB (39), the total uptake by retina and brain was lower than the lipophilicity trend line, suggesting that T_4 undergoes efflux transport at the BRB and BBB. Kassem *et al.* reported that P-gp is involved in the distribution of T_4 in the choroid plexus (40). It appears that [^{125}I]T_4 undergoes efflux by P-gp at the BRB and BBB, even although oatp1c1 exhibits influx transport of T_4 at the BBB. The RUI and BUI values of [^{3}H]digoxin and [^{3}H]vincristin, which are substrates for P-gp (41,42), were lower than the lipophilicity trend line, and the RUI and BUI values of [^{3}H]digoxin were increased in the presence of 5 mM verapamil, a P-gp inhibitor (Table II) (43). P-gp is expressed on the luminal membrane of the inner BRB and BBB and acts as an efflux transporter for lipophilic substrates undergoing freely diffuse to endothelial cells (2,41). No explanation is available at this time for the observed disparity in [^{3}H]verapamil uptake by the retina and brain across the BRB and BBB, respectively (Fig. 3). Although verapamil is a substrate of P-gp (44), it is also most likely a substrate of an unknown novel cationic transporter which carries out influx transport at the outer BRB (45). Therefore, verapamil uptake by the retina is greater than the lipophilicity trend line, and another reason is that P-gp is less active at the BRB than the BBB, since the BUI value of [^{3}H]digoxin is smaller than the RUI value (Table I). Further studies are needed to identify a transporter for verapamil transport at the BRB.

OAT3 is expressed on the abluminal membrane of the inner BRB and BBB, and MRP4 and AGCG2 are expressed on the luminal membrane of the inner BRB and BBB (9–11,46–48). PAH, which is a substrate for OAT3 and MRP4, undergoes efflux from retina and brain to blood most likely via OAT3 and MRP4 at the inner BRB and BBB after vitreous or brain injection (9,49,50). The RUI and BUI values of PAH were almost the same as that of D-mannitol (Table I). Thus, uptake of organic anions from blood by the luminal membrane of the BRB and BBB is small, and the role of efflux transporters for organic anions cannot be estimated using the carotid artery injection method.

In conclusion, the present study demonstrates that the BRB permeability for the passive diffusion of compounds is correlated with their lipophilic properties as is the BBB permeability. The lipophilicity trend line estimated from the RUI and DC values is an indication of the transport of drugs across the BRB. The substrates of influx transporters and P-gp have a greater and smaller BRB permeability, respectively, than the lipophilicity trend line. However, verapamil, which is a substrate of P-gp, has a greater RUI value than the lipophilicity trend line, but this is not the case for the BUI. Verapamil transport is different at the BRB and BBB, and a pharmacological evaluation of such differences may contribute to improving our understanding of the delivery of drugs to the retina and brain.

ACKNOWLEDGEMENTS

The authors thank Dr. M. Tomi, Mr. M. Okamoto, and Miss Y. Ohkura for technical assistance. This study was supported, in part, by a Grant-in-Aid for Scientific Research from the Japan Society for the Promotion of Science (JSPS).

REFERENCES

1. Cunha-Vaz JG. The blood-retinal barriers system. Basic concepts and clinical evaluation. Exp Eye Res. 2004;78:715–21.
2. Hosoya K, Tomi M. Advances in the cell biology of transport via the inner blood-retinal barrier: establishment of cell lines and transport functions. Biol Pharm Bull. 2005;28:1–8.
3. Stewart PA, Tuor UI. Blood-eye barriers in the rat: correlation of ultrastructure with function. J Comp Neurol. 1994;340:566–76.
4. Hosoya K, Tachikawa M. Inner blood-retinal barrier transporters: role of retinal drug delivery. Pharm Res. 2009;26:2055–65.
5. Takata K, Kasahara T, Kasahara M, Ezaki O, Hirano H. Ultracytochemical localization of the erythrocyte/HepG2-type glucose transporter (GLUT1) in cells of the blood-retinal barrier in the rat. Invest Ophthalmol Vis Sci. 1992;33:377–83.
6. Ohkura Y, Akanuma S, Tachikawa M, Hosoya K. Blood-to-retina transport of biotin via Na(+)-dependent multivitamin transporter (SMVT) at the inner blood-retinal barrier. Exp Eye Res. 2010;91:387–92.
7. Tomi M, Mori M, Tachikawa M, Katayama K, Terasaki T, Hosoya K. L-type amino acid transporter 1-mediated L-leucine transport at the inner blood-retinal barrier. Invest Ophthalmol Vis Sci. 2005;46:2522–30.
8. Tomi M, Kitade N, Hirose S, Yokota N, Akanuma S, Tachikawa M, *et al.* Cationic amino acid transporter 1-mediated L-arginine transport at the inner blood-retinal barrier. J Neurochem. 2009;111:716–25.
9. Hosoya K, Makihara A, Tsujikawa Y, Yoneyama D, Mori S, Terasaki T, *et al.* Roles of inner blood-retinal barrier organic anion transporter 3 in the vitreous/retina-to-blood efflux transport of p-aminohippuric acid, benzylpenicillin, and 6-mercaptopurine. J Pharmacol Exp Ther. 2009;329:87–93.
10. Tagami M, Kusuhara S, Honda S, Tsukahara Y, Negi A. Expression of ATP-binding cassette transporters at the inner blood-retinal barrier in a neonatal mouse model of oxygen-induced retinopathy. Brain Res. 2009;1283:186–93.
11. Asashima T, Hori S, Ohtsuki S, Tachikawa M, Watanabe M, Mukai C, *et al.* ATP-binding cassette transporter G2 mediates the efflux of phototoxins on the luminal membrane of retinal capillary endothelial cells. Pharm Res. 2006;23:1235–42.
12. Kadam RS, Kompella UB. Influence of lipophilicity on drug partitioning into sclera, choroid-retinal pigment epithelium, retina, trabecular meshwork, and optic nerve. J Pharmacol Exp Ther. 2010;332:1107–20.
13. Cornford EM. The blood-brain barrier, a dynamic regulation interface. Mol Physiol. 1985;7:219–59.
14. Pardridge WM, Triguero D, Yang J, Cancilla PA. Comparison of *in vitro* and *in vivo* models of drug transcytosis through the blood-brain barrier. J Pharmacol Exp Ther. 1990;253:884–91.
15. Levin VA. Relationship of octanol/water partition coefficient and molecular weight to rat brain capillary permeability. J Med Chem. 1980;23:682–4.
16. Alm A, Törnquist P. The uptake index method applied to studies on the blood-retinal barrier. I. A methodological study. Acta Physiol Scand. 1981;113:73–9.
17. Törnquist P, Alm A. Carrier-mediated transport of amino acids through the blood-retinal and the blood-brain barriers. Graefes Arch Clin Exp Ophthalmol. 1986;224:21–5.
18. Pardridge WM, Fierer G. Blood-brain barrier transport of butanol and water relative to N-isopropyl-p-iodoamphetamine as the internal reference. J Cereb Blood Flow Metab. 1985;5:275–81.
19. Pardridge WM, Mietus LJ, Frumar AM, Davidson BJ, Judd HL. Effects of human serum on transport of testosterone and estradiol into rat brain. Am J Physiol. 1980;239:E103–8.
20. Crone C. The permeability of capillaries in various organs as determined by use of the "indicator diffusion" method. Acta Physiol Scand. 1963;58:292–305.
21. Puchowicz MA, Xu K, Magness D, Miller C, Lust WD, Kern TS, *et al.* Comparison of glucose influx and blood flow in retina and brain of diabetic rats. J Cereb Blood Flow Metab. 2004;24:449–57.
22. Pardridge WM, Mietus LJ. Transport of steroid hormones through the rat blood-brain barrier. Primary role of albumin-bound hormone. J Clin Invest. 1979;64:145–54.
23. Nagase K, Tomi M, Tachikawa M, Hosoya K. Functional and molecular characterization of adenosine transport at the rat inner blood-retinal barrier. Biochim Biophys Acta. 2006;1758:13–9.
24. Okamoto M, Akanuma S, Tachikawa M, Hosoya K. Characteristics of glycine transport across the inner blood-retinal barrier. Neurochem Int. 2009;55:789–95.
25. Tachikawa M, Takeda Y, Tomi M, Hosoya K. Involvement of OCTN2 in the transport of acetyl-L-carnitine across the inner blood-retinal barrier. Invest Ophthalmol Vis Sci. 2010;51:430–6.
26. Stoll J, Wadhwani KC, Smith QR. Identification of the cationic amino acid transporter (System y+) of the rat blood-brain barrier. J Neurochem. 1993;60:1956–9.
27. Boado RJ, Li JY, Nagaya M, Zhang C, Pardridge WM. Selective expression of the large neutral amino acid transporter at the blood-brain barrier. Proc Natl Acad Sci USA. 1999;96:12079–84.
28. Yoneyama D, Shinozaki Y, Lu WL, Tomi M, Tachikawa M, Hosoya K. Involvement of system A in the retina-to-blood transport of l-proline across the inner blood-retinal barrier. Exp Eye Res. 2010;90:507–13.
29. Bleeker GM, van Haeringen NJ, Maas ER, Glasius E. Selective properties of the vitreous barrier. Exp Eye Res. 1968;7:37–46.
30. Ennis SR, Betz AL. Sucrose permeability of the blood-retinal and blood-brain barriers. Effects of diabetes, hypertonicity, and iodate. Invest Ophthalmol Vis Sci. 1986;27:1095–102.
31. Pardridge WM, Boado RJ, Farrell CR. Brain-type glucose transporter (GLUT-1) is selectively localized to the blood-brain

barrier. Studies with quantitative western blotting and *in situ* hybridization. J Biol Chem. 1990;265:18035–40.
32. Park S, Sinko PJ. The blood-brain barrier sodium-dependent multivitamin transporter: a molecular functional *in vitro-in situ* correlation. Drug Metab Dispos. 2005;33:1547–54.
33. Bodis-Wollner I. Visual electrophysiology in Parkinson's disease: PERG, VEP and visual P300. Clin Electroencephalogr. 1997;28:143–7.
34. Bhaskar PA, Vanchilingam S, Bhaskar EA, Devaprabhu A, Ganesan RA. Effect of L-dopa on visual evoked potential in patients with Parkinson's disease. Neurology. 1986;36:1119–21.
35. Kageyama T, Nakamura M, Matsuo A, Yamasaki Y, Takakura Y, Hashida M, *et al.* The 4F2hc/LAT1 complex transports L-DOPA across the blood-brain barrier. Brain Res. 2000;879:115–21.
36. Roth S, Rosenbaum PS, Osinski J, Park SS, Toledano AY, Li B, *et al.* Ischemia induces significant changes in purine nucleoside concentration in the retina-choroid in rats. Exp Eye Res. 1997;65:771–9.
37. Isakovic AJ, Abbott NJ, Redzic ZB. Brain to blood efflux transport of adenosine: blood-brain barrier studies in the rat. J Neurochem. 2004;90:272–86.
38. Forrest D, Reh TA, Rüsch A. Neurodevelopmental control by thyroid hormone receptors. Curr Opin Neurobiol. 2002;12:49–56.
39. Sugiyama D, Kusuhara H, Taniguchi H, Ishikawa S, Nozaki Y, Aburatani H, *et al.* Functional characterization of rat brain-specific organic anion transporter (Oatp14) at the blood-brain barrier: high affinity transporter for thyroxine. J Biol Chem. 2003;278:43489–95.
40. Kassem NA, Deane R, Segal MB, Chen R, Preston JE. Thyroxine (T4) transfer from CSF to choroid plexus and ventricular brain regions in rabbit: contributory role of P-glycoprotein and organic anion transporting polypeptides. Brain Res. 2007;1181:44–50.
41. Schinkel AH, Wagenaar E, van Deemter L, Mol CA, Borst P. Absence of the mdr1a P-Glycoprotein in mice affects tissue distribution and pharmacokinetics of dexamethasone, digoxin, and cyclosporin A. J Clin Invest. 1995;96:1698–705.
42. Tsuji A, Terasaki T, Takabatake Y, Tenda Y, Tamai I, Yamashima T, *et al.* P-glycoprotein as the drug efflux pump in primary cultured bovine brain capillary endothelial cells. Life Sci. 1995;51:1427–37.
43. Clarke G, O'Mahony SM, Cryan JF, Dinan TG. Verapamil in treatment resistant depression: a role for the P-glycoprotein transporter? Hum Psychopharmacol. 2009;24:217–23.
44. Bankstahl JP, Kuntner C, Abrahim A, Karch R, Stanek J, Wanek T, *et al.* Tariquidar-induced P-glycoprotein inhibition at the rat blood-brain barrier studied with (R)-11C-verapamil and PET. J Nucl Med. 2008;49:1328–35.
45. Han YH, Sweet DH, Hu DN, Pritchard JB. Characterization of a novel cationic drug transporter in human retinal pigment epithelial cells. J Pharmacol Exp Ther. 2001;296:450–7.
46. Mori S, Takanaga H, Ohtsuki S, Deguchi T, Kang YS, Hosoya K, *et al.* Rat organic anion transporter 3 (rOAT3) is responsible for brain-to-blood efflux of homovanillic acid at the abluminal membrane of brain capillary endothelial cells. J Cereb Blood Flow Metab. 2003;23:432–40.
47. Leggas M, Adachi M, Scheffer GL, Sun D, Wielinga P, Du G, *et al.* Mrp4 confers resistance to topotecan and protects the brain from chemotherapy. Mol Cell Biol. 2004;24:7612–21.
48. Hori S, Ohtsuki S, Tachikawa M, Kimura N, Kondo T, Watanabe M, *et al.* Functional expression of rat ABCG2 on the luminal side of brain capillaries and its enhancement by astrocyte-derived soluble factor(s). J Neurochem. 2004;90:526–36.
49. Smeets PH, van Aubel RA, Wouterse AC, van den Heuvel JJ, Russel FG. Contribution of multidrug resistance protein 2 (MRP2/ABCC2) to the renal excretion of p-aminohippurate (PAH) and identification of MRP4 (ABCC4) as a novel PAH transporter. J Am Soc Nephrol. 2004;15:2828–35.
50. Kakee A, Terasaki T, Sugiyama Y. Selective brain to blood efflux transport of para-aminohippuric acid across the blood-brain barrier: *in vivo* evidence by use of the brain efflux index method. J Pharmacol Exp Ther. 1997;283:1018–25.